A study of code uncertainty in stochastic model updating with Kriging.

Peng Liang[1], John E Mottershead[1,2] and F.A. DiazDelaO[1,2]
[1] Centre for Engineering Dynamics, University of Liverpool
Liverpool, L69 3GH, UK
[2] Institute for Risk and Uncertainty, University of Liverpool
Liverpool, L69 3GH, UK
e-mail: **j.e.mottershead@liverpool.ac.uk**

Abstract

The Kriging predictor is regularly used as a surrogate (or *emulator*) to reduce the cost of forward propagation of uncertainty. Such surrogates can be expensive to develop with the required fidelity to a physics-based model (or *simulator*), such as finite elements. The unknown closeness of the emulator to the simulator is known as *code uncertainty*, the treatment of which is addressed in this paper. The Kriging approach provides a probabilistic model of code uncertainty which may be used within a validation process for the assessment of accuracy. The problem with this approach is that it depends entirely upon the forward propagation of uncertainty and takes no account of the effect of uncertainty on the input (parameters) when determined by an inverse process such as stochastic model updating. A preliminary deterministic FE update is shown to lead to a new two-stage stochastic model updating procedure for the elimination of code uncertainty to render the updated model representative of physical variability. In addition, a resampling technique is introduced to allow an assessment of the closeness of alternative functions in the input space to the most probable function returned as the mean of a Gaussian random process by Kriging.

1 Introduction

Surrogate models [1], being 'models of models' are now well established especially in the field of engineering design optimisation. The reason for using them is that physical models, typically finite element (FE) models, used in industry have become so large and complicated that their use in design optimisation is prohibitively expensive. Of course, to create a less expensive model of a detailed and expensive physical model involves unknown uncertainty, which must be modelled statistically. Thus, in general surrogates are small-scale statistical models used to represent large-scale deterministic ones.

The fact that surrogates are approximations means that great care must be taken in their construction to ensure that the important features of the original model are retained. This is not an inexpensive procedure [2]. First a sufficiently large number of training solutions using the full physical model must be completed, and this should be followed by an even larger number of validation test runs, away from the training points, to ensure that the surrogate is sufficiently accurate across the region of interest. One way to reduce the cost of this process is to represent the full model not by a single (global) surrogate, but by a number of different local surrogates with high fidelity in chosen regions of the design space [3].

Gano et al. [4] compared the performance of three surrogate modelling techniques; a commercial code known as 'Datascape', Kriging and second-order regression. They found that the Kriging method, now in widespread use in research and also in industry, was the best performing approach only for the case of sparse (well separated) training samples used to build the model. There are in fact a number of potential problems that can affect the performance a Kriging model: (1) training samples that are too close together can cause the output correlation matrix to become numerically singular, (2) maximum likelihood estimation of certain Kriging parameters is expensive and often beset with problems of multimodality and long ridges [5]. These problems are exacerbated for multi-parameter large scale models to the extent that

it may become impossible to construct a Kriging model, usually because a converged solution for the Kriging parameters cannot be obtained.

Applications of Kriging models in engineering dynamics include [6-8]. In FE model updating Kriging has been implemented in an interval-based approach [9, 10]. Also the use of surrogates is essential in Bayesian model updating [11, 12] requiring multiple solutions for Markov-chain Monte-Carlo analysis using modern variants of the Metropolis-Hastings algorithm. One advantage of the Kriging approach is that it provides a model of code uncertainty [13] in the form of a Gaussian random process to represent the unknown closeness of the emulator function to the input-output function of the simulator. The exploitation of this coding uncertainty model does not seem to have been fully considered especially in the case of finite element model updating.

In this paper an experimental example is used illustrate a new two-stage approach to stochastic model updating with the Kriging predictor. The usual approach to training a Kriging model is based entirely upon the forward propagation of uncertainty and is deemed to be good enough by the satisfaction of validation criteria at chosen points, away from the training points. The mean model then obtained is the most probable model. However, model updating is an inverse process whereby the statistics of uncertain parameters are determined from observed output variability. This provides a new opportunity to judge the performance of the trained Kriging model not only in replicating FE outputs but in identifying input (parameter) uncertainty.

At the training points the Kriging model represents the FE model exactly, but away from these points the Gaussian process admits multiple solutions (alternative functions that also pass through zero at the training points). O'Hagan [13] produced a histogram of the mean outputs from each such solution. The approach presented here is somewhat similar, except that instead of considering alternative output functions the Gaussian process is projected onto the input (parameter) space by a local sensitivity approach - this allows the investigation of alternative input functions. Each resampling of such alternative input functions allows a new set of means and covariances to be determined. The variability (e.g. standard deviation) of these statistics can be determined after re-sampling has been carried out a sufficiently large number of times

The two-stage approach described in the paper enables an assessment of trained Kriging models based upon both output and input (parameter) uncertainty. First, a preliminary deterministic updating of the FE model should be carried out to remove any modelling errors not attributable to variability. This is the point at which the Kriging model should be trained and is carried out in two stages. Stage 1 consists of training a Kriging model and carrying out stochastic model updating using synthetic data from the updated FE model. Any lack of agreement between the FE outputs and those obtained from the updated Kriging model is represented by code uncertainty. Stage 2 takes place after the code uncertainty has been sufficiently eliminated, by including, if necessary, a number of additional training points. It consists of a second round of stochastic model updating, this time using the experimental outputs, and since code uncertainty was effectively removed at the first stage, the only errors present are due to inaccurate modelling of the randomised parameters.

2. Kriging predictor mean and sensitivity

For a full and discursive account of the Kriging methodology the reader is referred to the works of Sacks et al [14] and Bastos and O'Hagan [15]. A brief overview will now be presented.

Given a simulator process with output vector $\mathbf{z}(\boldsymbol{\theta}) = \left[z_1, z_2, \cdots, z_{n_{out}} \right]^T$ and inputs $\boldsymbol{\theta} = \left[\theta_1, \theta_2, \cdots, \theta_{n_{in}} \right]^T$, a Kriging predictor may be constructed with n_s design points $\left\{\boldsymbol{\theta}^{(1)}, \mathbf{z}^{(1)}\right\}, \left\{\boldsymbol{\theta}^{(2)}, \mathbf{z}^{(2)}\right\}, \cdots, \left\{\boldsymbol{\theta}^{(n_s)}, \mathbf{z}^{(n_s)}\right\}$ observed from the simulator. The mean Kriging prediction is generally written in the form [9, 16],

$$\overline{\mathbf{z}} = \mathbf{B}^T \mathbf{f}\left(\boldsymbol{\theta}\right) + \boldsymbol{\Lambda}\, \mathbf{r}\left(\boldsymbol{\theta}\right) \tag{1}$$

The first right-hand-side term $\mathbf{B}^T \mathbf{f}(\boldsymbol{\theta})$ may take the form of a regression model and the second term $\boldsymbol{\Lambda}\mathbf{r}(\boldsymbol{\theta})$ is an assumed white-noise expression representing the approximation error for each component of the

output in the region of interest [16]. As part of first term, $\mathbf{f}=\left[\, f_0, f_1, \cdots, f_{n_f} \,\right]^{\mathrm{T}}$ is a vector of regression features, where f_0 is unity and n_f denotes the number of features in addition to f_0. For example, in the case of a 2nd order polynomial regression with 2 inputs θ_1 and θ_2, $\mathbf{f}$ might be given by $\mathbf{f}=\left[1,\theta_1,\theta_2,\theta_1^2,\theta_1\theta_2,\theta_2^2\right]^{\mathrm{T}}$. The matrix $\mathbf{B}=\begin{bmatrix}\boldsymbol{\beta}_0^T\\ \boldsymbol{\beta}_1^T\\ \vdots\\ \boldsymbol{\beta}_{n_f}^T\end{bmatrix}_{(n_f+1)\times n_{out}}$ where,

$$\mathbf{F}_s^T\mathbf{B}=\mathbf{Z}_s^T \tag{2}$$

$$\mathbf{F}_s=\left(\mathbf{f}\left(\boldsymbol{\theta}^{(1)}\right)\quad \mathbf{f}\left(\boldsymbol{\theta}^{(2)}\right)\quad \cdots\quad \mathbf{f}\left(\boldsymbol{\theta}^{(n_s)}\right)\right);\quad \mathbf{Z}_s=\left(\mathbf{z}^{(1)}\quad \mathbf{z}^{(2)}\quad \cdots\quad \mathbf{z}^{(n_s)}\right)^T;\quad n_s \succ n_f+1 \tag{3}$$

In the second right-hand-side term of equation (1), $\mathbf{r}(\boldsymbol{\theta})$ is a vector of output correlations between an arbitrary point and a design point,

$$\mathbf{r}(\boldsymbol{\theta})=\begin{bmatrix}r^{(1)}\\ r^{(2)}\\ \vdots\\ r^{(n_s)}\end{bmatrix}_{n_s\times 1}=\begin{bmatrix}C\left(\boldsymbol{\theta},\boldsymbol{\theta}^{(1)}\right)\\ C\left(\boldsymbol{\theta},\boldsymbol{\theta}^{(2)}\right)\\ \vdots\\ C\left(\boldsymbol{\theta},\boldsymbol{\theta}^{(n_s)}\right)\end{bmatrix} \tag{4}$$

In the case of two arbitrary input vectors $\boldsymbol{\theta}_u$ and $\boldsymbol{\theta}_v$ the correlation between outputs $\mathbf{z}_u$ and $\mathbf{z}_v$ may be expressed in the general form,

$$C\left(\boldsymbol{\theta}_u,\boldsymbol{\theta}_v,\boldsymbol{\zeta}\right)=\prod_{i=1}^{n_{in}} C_i\left(\theta_{u_i},\theta_{v_i},\boldsymbol{\zeta}\right) \tag{5}$$

and in particular in the research described in this paper,

$$C_i\left(\theta_{u_i},\theta_{v_i},\zeta_i\right)=\exp\left(-\zeta_i\left(\theta_{u_i}-\theta_{v_i}\right)^2\right) \tag{6}$$

where ζ_i is a correlation parameter.

The matrix $\boldsymbol{\Lambda}$ may be written in expanded form as,

$$\boldsymbol{\Lambda}=\left[\mathbf{Z}_s-\mathbf{B}^{\mathrm{T}}\mathbf{F}_s\right]\mathbf{R}^{-1} \tag{7}$$

where **R** is the design-point correlation matrix,

$$\mathbf{R}=\begin{bmatrix}C(\boldsymbol{\theta}^{(1)},\boldsymbol{\theta}^{(1)}) & C(\boldsymbol{\theta}^{(2)},\boldsymbol{\theta}^{(1)}) & \cdots & C(\boldsymbol{\theta}^{(n_s)},\boldsymbol{\theta}^{(1)})\\ C(\boldsymbol{\theta}^{(1)},\boldsymbol{\theta}^{(2)}) & C(\boldsymbol{\theta}^{(2)},\boldsymbol{\theta}^{(2)}) & \cdots & C(\boldsymbol{\theta}^{(n_s)},\boldsymbol{\theta}^{(2)})\\ \vdots & \vdots & \ddots & \vdots\\ C(\boldsymbol{\theta}^{(1)},\boldsymbol{\theta}^{(n_s)}) & C(\boldsymbol{\theta}^{(2)},\boldsymbol{\theta}^{(n_s)}) & \cdots & C(\boldsymbol{\theta}^{(n_s)},\boldsymbol{\theta}^{(n_s)})\end{bmatrix}_{n_s\times n_s} \tag{8}$$

Matrices **B** and **Λ** are fully determined by the fixed set of design points $\left\{\boldsymbol{\theta}^{(1)},\mathbf{z}^{(1)}\right\},\left\{\boldsymbol{\theta}^{(2)},\mathbf{z}^{(2)}\right\},\cdots,\left\{\boldsymbol{\theta}^{(n_s)},\mathbf{z}^{(n_s)}\right\}$. Therefore, in the expression of the predictor mean, only $\mathbf{f}(\boldsymbol{\theta})$ and $\mathbf{r}(\boldsymbol{\theta})$ are functions of input $\boldsymbol{\theta}$.

Expansion of the Kriging model in a Taylor series truncated after the first-order derivative term leads to the sensitivity matrix,

$$\mathbf{S}=\begin{bmatrix} \frac{\partial \overline{z}_1}{\partial \theta_1} & \frac{\partial \overline{z}_1}{\partial \theta_2} & \cdots & \frac{\partial \overline{z}_1}{\partial \theta_{n_{in}}} \\ \frac{\partial \overline{z}_2}{\partial \theta_1} & \frac{\partial \overline{z}_2}{\partial \theta_2} & \cdots & \frac{\partial \overline{z}_2}{\partial \theta_{n_{in}}} \\ \vdots & \vdots & & \vdots \\ \frac{\partial \overline{z}_{n_{out}}}{\partial \theta_1} & \frac{\partial \overline{z}_{n_{out}}}{\partial \theta_2} & \cdots & \frac{\partial \overline{z}_{n_{out}}}{\partial \theta_{n_{in}}} \end{bmatrix} \tag{9}$$

such that,

$$\mathbf{S}=\frac{\partial \overline{\mathbf{z}}}{\partial \boldsymbol{\theta}}=\mathbf{B}^{\mathrm{T}}\frac{\partial \mathbf{f}}{\partial \boldsymbol{\theta}}+\boldsymbol{\Lambda}\frac{\partial \mathbf{r}}{\partial \boldsymbol{\theta}} \tag{10}$$

and the overbar denotes the mean. Then equation (10) may be re-written in expanded form,

$$\mathbf{S}=\mathbf{B}^{\mathrm{T}}\begin{bmatrix} \frac{\partial f_0}{\partial \theta_1} & \frac{\partial f_0}{\partial \theta_2} & \cdots & \frac{\partial f_0}{\partial \theta_{n_{in}}} \\ \frac{\partial f_1}{\partial \theta_1} & \frac{\partial f_1}{\partial \theta_2} & \cdots & \frac{\partial f_1}{\partial \theta_{n_{in}}} \\ \vdots & \vdots & & \vdots \\ \frac{\partial f_{n_f}}{\partial \theta_1} & \frac{\partial f_{n_f}}{\partial \theta_2} & \cdots & \frac{\partial f_{n_f}}{\partial \theta_{n_{in}}} \end{bmatrix}+\boldsymbol{\Lambda}\begin{bmatrix} \frac{\partial C(\theta,\theta^{(1)})}{\partial \theta_1} & \frac{\partial C(\theta,\theta^{(1)})}{\partial \theta_2} & \cdots & \frac{\partial C(\theta,\theta^{(1)})}{\partial \theta_{n_{in}}} \\ \frac{\partial C(\theta,\theta^{(2)})}{\partial \theta_1} & \frac{\partial C(\theta,\theta^{(2)})}{\partial \theta_2} & \cdots & \frac{\partial C(\theta,\theta^{(2)})}{\partial \theta_{n_{in}}} \\ \vdots & \vdots & & \vdots \\ \frac{\partial C(\theta,\theta^{(n_s)})}{\partial \theta_1} & \frac{\partial C(\theta,\theta^{(n_s)})}{\partial \theta_2} & \cdots & \frac{\partial C(\theta,\theta^{(n_s)})}{\partial \theta_{n_{in}}} \end{bmatrix} \tag{11}$$

3. The Kriging prediction variance

For reasons of simplicity, in this sub-section, a single term $z(\boldsymbol{\theta})$ of an arbitrarily chosen output vector is used to explain the Kriging prediction variance. Then a random vector $\left[z,\mathbf{z}_s^T\right]^T$ is defined where $\mathbf{z}_s=\left[z^{(1)},z^{(2)},\cdots,z^{(n_s)}\right]^T$ is the vector of design-points outputs. It is clear that $\mathbf{z}_s$ is a constant vector, not a function of $\boldsymbol{\theta}$, because the design points are fixed. To be more precise, $\mathbf{z}_s=\left[z\left(\boldsymbol{\theta}^{(1)}\right),z\left(\boldsymbol{\theta}^{(2)}\right),\cdots,z\left(\boldsymbol{\theta}^{(n_s)}\right)\right]^T$, the response of the Kriging predictor at design points parameters $\boldsymbol{\theta}^{(1)},\boldsymbol{\theta}^{(2)},\cdots,\boldsymbol{\theta}^{(n_s)}$. The choice of correlation function (5) and (6) ensures that the prediction mean of the Kriging predictor with noisy-free observations exactly passes through the design points $\left\{\boldsymbol{\theta}^{(1)},\mathbf{z}^{(1)}\right\},\left\{\boldsymbol{\theta}^{(2)},\mathbf{z}^{(2)}\right\},\cdots,\left\{\boldsymbol{\theta}^{(n_s)},\mathbf{z}^{(n_s)}\right\}$. Therefore, we replace $\mathbf{z}(\boldsymbol{\theta}_s)$ with the simpler notation $\mathbf{z}_s$ in what follows.

It may be shown [17, 18] that the conditional probability $p\left(z(\boldsymbol{\theta})\middle|z_s,\boldsymbol{\beta},\sigma^2\right)\sim\mathcal{N}\left(\overline{z},\sigma^2C_1(\boldsymbol{\theta},\boldsymbol{\theta})\right)$ where,

$$\overline{z}(\boldsymbol{\theta})=\boldsymbol{\beta}^T\mathbf{f}(\boldsymbol{\theta})+\mathbf{r}(\boldsymbol{\theta})^T\mathbf{R}^{-1}\left(\mathbf{z}_s-\mathbf{F}_s^T\boldsymbol{\beta}\right) \tag{12}$$

and,

$$C_1(\boldsymbol{\theta}_u,\boldsymbol{\theta}_v)=C(\boldsymbol{\theta}_u,\boldsymbol{\theta}_v)-\mathbf{r}(\boldsymbol{\theta}_u)^T\mathbf{R}^{-1}\mathbf{r}(\boldsymbol{\theta}_v) \tag{13}$$

Then by removing the conditioning on $\boldsymbol{\beta}$ and σ^2 it is found that $p\left(z\middle|\mathbf{z}_s\right)\sim\mathcal{N}\left(\overline{z},\sigma^2C_2(\boldsymbol{\theta},\boldsymbol{\theta})\right)$ where $\overline{z}$ is given by

$$\bar{z}(\boldsymbol{\theta}) = \hat{\boldsymbol{\beta}}^T \mathbf{f}(\boldsymbol{\theta}) + \mathbf{r}(\boldsymbol{\theta})^T \mathbf{R}^{-1}\left(\mathbf{z}_s - \mathbf{F}_s^T \hat{\boldsymbol{\beta}}\right) \tag{14}$$

and,

$$C_2(\boldsymbol{\theta}_u, \boldsymbol{\theta}_v) = C_1(\boldsymbol{\theta}_u, \boldsymbol{\theta}_v) + \left(\mathbf{f}(\boldsymbol{\theta}_u)^T - \mathbf{r}(\boldsymbol{\theta}_u)^T \mathbf{R}^{-1}\mathbf{F}_s^T\right)\left(\mathbf{F}_s\mathbf{R}^{-1}\mathbf{F}_s^T\right)^{-1}\left(\mathbf{f}(\boldsymbol{\theta}_v)^T - \mathbf{r}(\boldsymbol{\theta}_v)^T \mathbf{R}^{-1}\mathbf{F}_s^T\right)^T \tag{15}$$

Finally, by combining equations (13) and (15) it is found that,

$$\begin{aligned} C_2(\boldsymbol{\theta}_u, \boldsymbol{\theta}_v) = C(\boldsymbol{\theta}_u, \boldsymbol{\theta}_v) + \left(\mathbf{f}(\boldsymbol{\theta}_u)^T - \mathbf{r}(\boldsymbol{\theta}_u)^T \mathbf{R}^{-1}\mathbf{F}_s^T\right)\left(\mathbf{F}_s\mathbf{R}^{-1}\mathbf{F}_s^T\right)^{-1} \\ \times\left(\mathbf{f}(\boldsymbol{\theta}_v)^T - \mathbf{r}(\boldsymbol{\theta}_v)^T \mathbf{R}^{-1}\mathbf{F}_s^T\right)^T - \mathbf{r}(\boldsymbol{\theta}_u)^T \mathbf{R}^{-1}\mathbf{r}(\boldsymbol{\theta}_v) \end{aligned} \tag{16}$$

The hyper-parameters $\boldsymbol{\beta}$, σ^2 and ζ_i may be estimated by using a maximum likelihood approach,

$$\hat{\boldsymbol{\beta}} = \left(\mathbf{F}_s\mathbf{R}^{-1}\mathbf{F}_s^T\right)^{-1}\mathbf{F}_s\mathbf{R}^{-1}\mathbf{z}_s \tag{17}$$

$$\hat{\sigma}^2 = \frac{1}{n_s}\left(\mathbf{z}_s - \mathbf{F}_s^T\hat{\boldsymbol{\beta}}\right)^T \mathbf{R}^{-1}\left(\mathbf{z}_s - \mathbf{F}_s^T\hat{\boldsymbol{\beta}}\right) \tag{18}$$

where the denominator n_s should be replaced with $n_s - n_f - 1$ to obtain a central estimate of the variance [16]. The Kriging model represented by equations (14) and (16), conditional upon $\mathbf{z}_s$, may be improved (and the code uncertainty reduced) by increasing the number of sampling points. Having said that, the variance $\sigma^2 C_2(\boldsymbol{\theta},\boldsymbol{\theta})$ relates only to the mathematical construction of the Kriging model, completely unrelated the physical dependency that exists between the outputs. It is a measure of our 'degree of belief' in the Kriging mean value, for example if $p(\mathbf{z}(\boldsymbol{\theta})|\mathbf{z}_s)$ is sharply peaked we have greater confidence in the mean than if the PDF was shallow at $\boldsymbol{\theta}$.

4. Resampling

Probably the simplest approach conceptually to stochastic model updating would be to carry out multiple tests with measured output variability and then conduct a large number of deterministic updating runs (one for each individual output) to determine variability in chosen updating parameters. This expensive process is made inexpensive by the use of Kriging (or any other surrogate). The mean Kriging function, represented by the full black curve in Figure 1, is the most probable function fitted exactly through the training points in the multivariate output space of the updating parameters. Other functions, such as the black dashed curve, may be sampled from the random process $p(\mathbf{z}(\boldsymbol{\theta})|\mathbf{z}_s) \sim \mathcal{N}\left(\bar{\mathbf{z}}, \boldsymbol{\Sigma}_{\mathbf{z}(\theta)}\right)$; $\boldsymbol{\Sigma}_{\mathbf{z}(\theta)} = \mathrm{diag}\left[\sigma_1^2 C_2(\boldsymbol{\theta},\boldsymbol{\theta}), \cdots, \sigma_{n_{out}}^2 C_2(\boldsymbol{\theta},\boldsymbol{\theta})\right]$ and represent alternative, less probable functions. For reasons of simplicity Figure 1 illustrates the case of a single input and a single output.

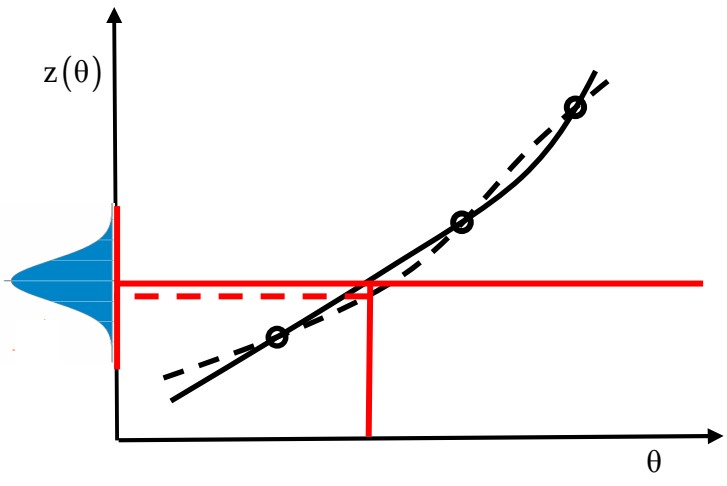

Figure 1. Output code uncertainty

In model updating, the objective is the determine uncertainty on the parameters. This can be achieved by projecting the output coding uncertainty, shown in Figure 1, onto the input space. This is illustrated in Figure 2.

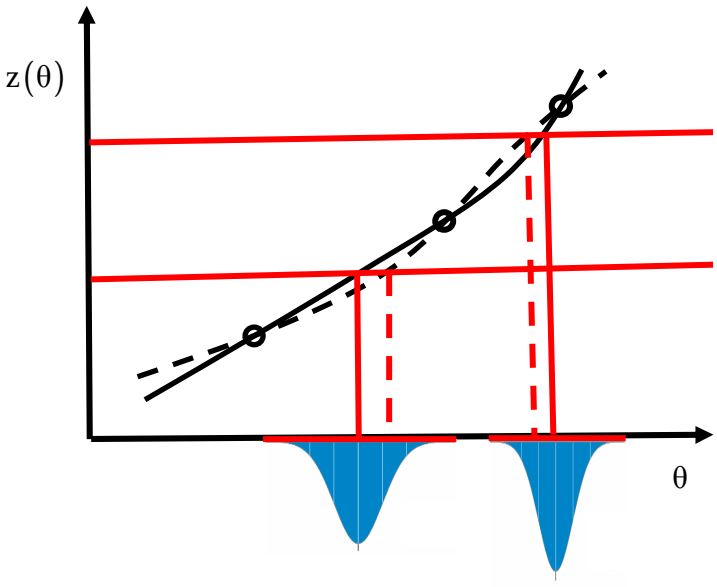

Figure 2. Input code uncertainty

The prediction variance $\boldsymbol{\Sigma}_{\boldsymbol{z}(\boldsymbol{\theta})}$ may be projected onto the input space with a local assumption of linearity at the point $\{\boldsymbol{\theta}, \mathbf{z}(\boldsymbol{\theta})\}$ on the prediction mean surface expressed by the Jacobian matrix, $\mathbf{J}_\theta = \frac{\partial \overline{\mathbf{z}}}{\partial \boldsymbol{\theta}} = \mathbf{S}_\theta$. Thus,

$$\boldsymbol{\Sigma}_{\boldsymbol{z}(\boldsymbol{\theta})} = \mathbf{S}_\theta \boldsymbol{\Sigma}_{\boldsymbol{\theta}} \mathbf{S}_\theta^T \tag{19}$$

so that by projection,

$$\boldsymbol{\Sigma}_\theta = \left[\mathbf{S}^T\mathbf{S}\right]_\theta^{-1} \mathbf{S}_\theta^T \boldsymbol{\Sigma}_{z(\theta)} \mathbf{S}_\theta \left[\mathbf{S}^T\mathbf{S}\right]_\theta^{-1} \tag{20}$$

Thus for every deterministic update, at every individual measurement, the parameter vector $\boldsymbol{\theta}$ has a distribution given by $\mathcal{N}\left(\overline{\boldsymbol{\theta}}, \boldsymbol{\Sigma}_\theta\right)$. Off-diagonal terms of the covariance matrix $\boldsymbol{\Sigma}_{\boldsymbol{z}(\boldsymbol{\theta})}$, between different outputs (typically different natural frequencies), do not exist in the present Kriging formulation so that only the diagonal terms are determined at arbitrary $\boldsymbol{\theta}$.

An investigation of input variability may then the carried out by resampling from this distribution $\mathcal{N}\left(\overline{\boldsymbol{\theta}}, \boldsymbol{\Sigma}_\theta\right)$. In this way a new parameter vector $\boldsymbol{\theta}^*$ may be obtained for each deterministics update (i.e. for each of the n_m individual measurements). These new inputs $\boldsymbol{\theta}^*$ and corresponding outputs $\mathbf{z}\left(\boldsymbol{\theta}^*\right)$, when assembled as $\left\{\left\{\boldsymbol{\theta}^*_{(1)}, \mathbf{z}_{(1)}\left(\boldsymbol{\theta}^*\right)\right\}, \left\{\boldsymbol{\theta}^*_{(2)}, \mathbf{z}_{(2)}\left(\boldsymbol{\theta}^*\right)\right\}, \cdots, \left\{\boldsymbol{\theta}^*_{(n_m)}, \mathbf{z}_{(n_m)}\left(\boldsymbol{\theta}^*\right)\right\}\right\}$ may be used to obtain new input and output means and covariance matrices. These resampled statistics represent another possible model within the Gaussian process, different from that of the most probable Kriging model.

This resampling procedure should be repeated a sufficient number of times to allow the quantification of variability on the new means and covariances of the updated model. If the standard deviations on the

means and covariances are relatively large then the Kriging model admits a wide range of possible updating solutions and vice-versa.

5. Modelling error and code uncertainty

The response of a mechanical system, typically a set of natural frequencies, is usually measured by experimental methods. A FE model of the system in question is built to simulate the response of the system numerically. And a surrogate is trained to represent the FE model economically. However, the measurement precision is imperfect, the model contains assumptions and inaccuracies and the surrogate does not reproduce the FE output perfectly. Thus,

Experiment measurements = True physical response + Measurement error

Finite element model output = True physical response + Modelling error (FE)

Kriging model output = Ture physical response + Modelling error (FE) + Code uncertainty (K)

where the letter K in brackets denotes the code uncertainty due to Kriging-model inaccuracy.

Based on the above expressions, it is clear that the result of model updating conducted with a Kriging model to match experiment measurements would be affected by measurement error, modelling error (FE) and code uncertainty (K). In what follows the measurement error is considered to be negligible.

6. Model updating procedure.

The problem is that of observed variability in measured output due to unknown randomness in system parameters. In addition to the random parameters there are other deterministic parameters inaccurately represented in the FE model. The purpose is to correct the FE model using a Kriging surrogate. The procedure shown in Figure 1 can be described as follows:

- Update the FE model to correct deterministic parameter inaccuracies.
- Create a Kriging model to represent randomness in the parameters.
- Step 1: Carry out stochastic model updating using the Kriging model and synthetic data from the previous (deterministically) updated FE model – the only errors present are represented by code uncertainty.
- Compare outputs from the stochastically updated model with the synthetic data.
- Repeat Step 1, each time introducing more training points, until the code uncertainty has disappeared sufficiently. The Kriging model is now fully trained and code uncertainty is effectivelyeliminated.
- Step 2: Carry out stochastic model updating using trained Kriging model and experimental data.
- The updated model is representative of physical variability without contamination by code uncertainty.

7. Experimental test structure.

The experimental aluminium frame used in the case study is shown in Figure 2. It was built with beams and movable mass blocks. The frame was fixed to a rigid base with four bolts and the mass blocks were machined with a ridge that formed a line of contact with the beams at the level of the centre of mass. The vertical position of movable mass could adjusted to represent structural variability while the horizontal (axis x) position remained unchanged. The mass centres of the two blocks were always on the vertical centre lines of the short vertical beams.

The natural frequencies of the frame are the measured outputs. The problem of randomness among nominally identical structure is then simulated by moving the two masses to different positions denoted by p_1 and p_2. The distance from the bottom horizontal beam to the lower mass is p_1 and that from the middle horizontal beam to the upper mass is p_2. We call the positions of two masses in one testing (p_1, p_2) a position pair. The overall height of frame was 80cm, and each short vertical beam is less than

40cm long due to the thickness of beams and the maximum feasible regions of variability of p_1 and p_2 was from 5cm to 35cm. In total 100 positional pairs (p_1, p_2) were designed artificially to follow a bivariate normal distribution with mean [20, 20] and covariance matrix $\begin{bmatrix} 9 & 0 \\ 0 & 9 \end{bmatrix}$. It is important to distinguish the physical distribution of mass positions from the distribution $\mathcal{N}\left(\bar{\boldsymbol{\theta}}, \boldsymbol{\Sigma}_\theta\right)$, obtained by projection of the Kriging-output Gaussian process onto the parameter space in equation (20). This latter distribution is a feature of the Kriging model unrelated to the physical distribution of mass positions.

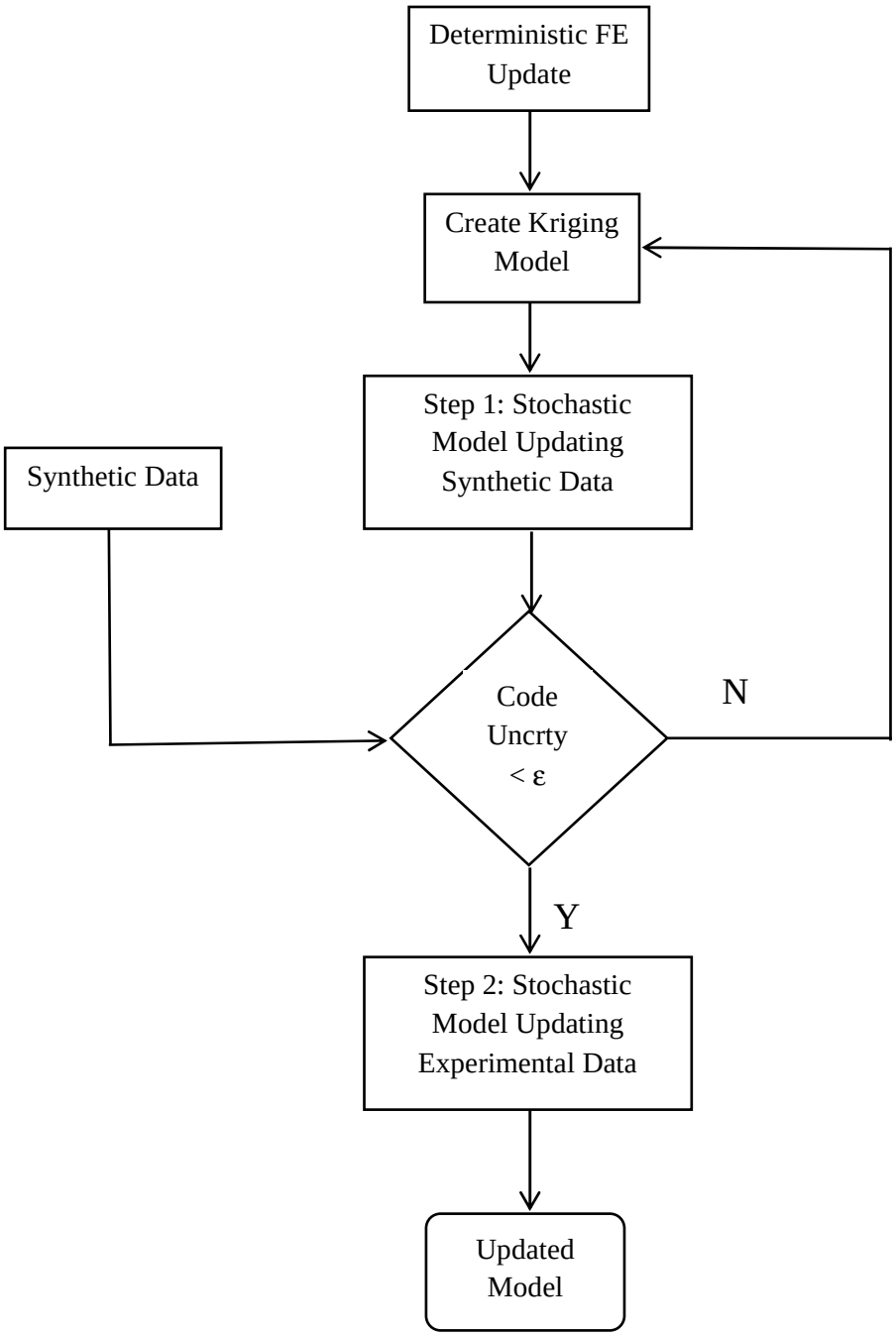

Figure 1. Stochastic model updating procedure

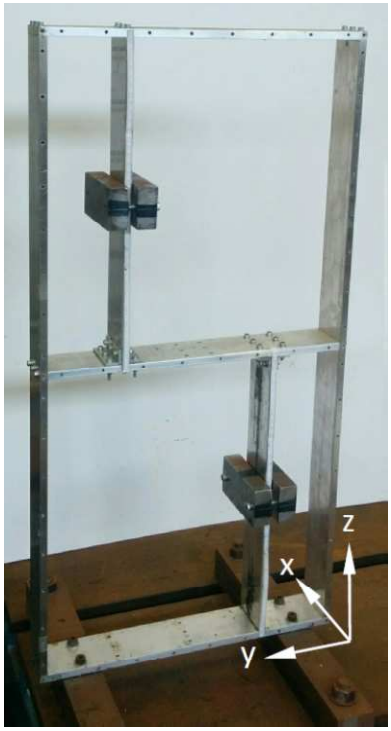

Figure 2. Experimental frame structure

8. Deterministic model updating

A finite element beam model was constructed to represent the frame with the ultimate purpose of producing a model that predicts the distribution of system natural frequencies without contamination by code uncertainty caused by the use of a Kriging surrogate. However, in addition to the deliberately introduced randomness (in known parameters) of the experiment, the model was not able to fully represent the detailed behaviour of the joints between the beams or the bolted connection to the rigid base. These modelling errors were entirely deterministic and their effect should be removed before applying stochastic model updating to determine the imposed random distribution on (p_1, p_2). This requires a preliminary deterministic FE update before training the Kriging model.

The deterministic model updating was carried out with mass blocks positioned in the middle and extreme locations, $(p_1, p_2) = (20,20), (5,5)$ and $(35,35)$. Six natural frequencies at each of the three configurations were selected as outputs, there being 18 in total. These were the natural frequencies of the 1st order in-plane bending, 1st order out-of-plane bending, 1st order torsion, 2nd order in-plane bending, 2nd order out-of-plane bending, and 2nd order torsion modes. Natural frequencies were measured by hammer impact testing, and five parameters were updated. These were as follows: (1) the shear modulus of the base beam to represent the effect of the bolted base connection on the out-of-plane bending and twisting mode, (2) the shear modulus of the two long vertical beams to represent the constraining effect of joints on the out-of-plane twisting modes, (3) the shear modulus of the lower short vertical beam which undergoes considerable twisting in the 3rd and 6th modes, and (4) and (5) the radii of gyration of the masses about the x and y axes. The six FE modes shown in Figure 3 were then in very good agreement with measured natural frequencies. In the central location agreement of less than 1% was obtained and at the extreme positions less than 2%. The FE predictions after model updating are shown in **Table 1**. Further details of the deterministic model updating can be found in the PhD this by the first author [19].

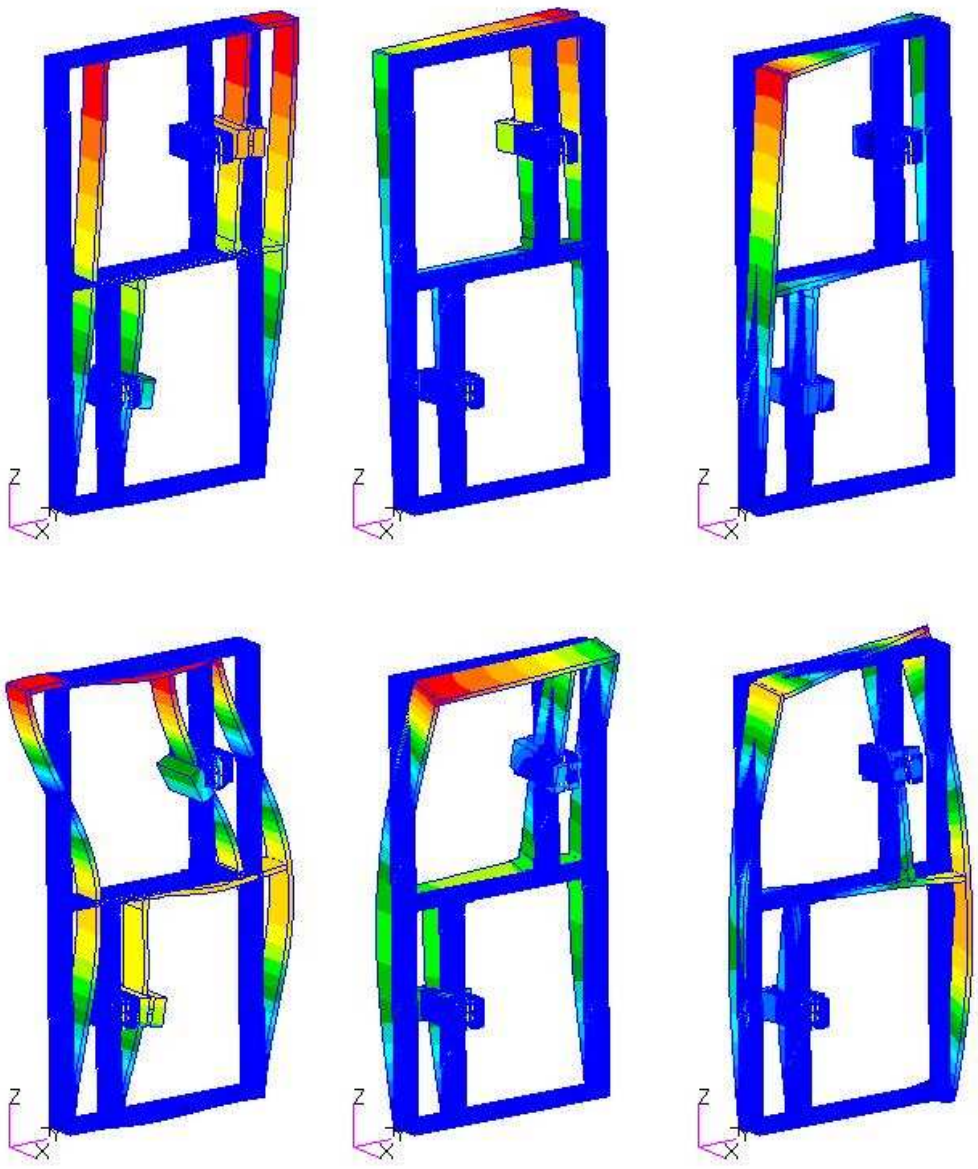

Figure 3: Mode shapes of 1st in-plane bending, 1st out-of-plane bending, 1st torsion, 2nd in-plane bending, 2nd out-of-plane bending, and 2nd torsion

Table 1: Beam model frequencies after model updating

		Experiment (Hz)	Beam element model after model updating (Hz)	Error
$(p_1, p_2) = (20, 20)$	f1	17.909	18.059	0.84%
	f2	20.277	20.154	-0.61%
	f3	45.674	45.264	-0.90%
	f4	64.727	65.217	0.76%
	f5	190.844	190.573	-0.14%
	f6	284.086	284.624	0.19%
(p_1, p_2)	f1	20.116	19.924	-0.95%

$= (5, 5)$	f2	22.792	22.669	-0.54%
	f3	47.520	47.167	-0.74%
	f4	63.955	63.460	-0.77%
	f5	183.823	181.060	-1.50%
	f6	283.511	279.852	-1.29%
(p_1, p_2) $= (35, 35)$	f1	15.952	15.998	0.29%
	f2	17.889	17.677	-1.19%
	f3	42.438	41.939	-1.18%
	f4	50.659	50.800	0.28%
	f5	163.553	166.342	1.71%
	f6	257.823	257.058	-0.30%

9. Step 1: Stochastic model updating and resampling from synthetic data

A 9-design point and a 49-design point Kriging model were constructed using the MATLAB Kriging toolbox, 'DACE' [16], with inputs p_1 and p_2 and six frequencies $f_1, f_2, \ldots, f_6$ as outputs. A Gaussian correlation function was used. Inputs p_1 and p_2 became the updating parameters for stochastic model updating with the six natural frequencies $f_1, f_2, \ldots, f_6$ as outputs. The locations of design points were arranged in full factorial design in the feasible domain $p_1, p_2 \in [5, 35]$ with 3 levels and 7 levels respectively, making 9-point and 49-point designs respectively. Contour plots of the six natural frequencies, as functions of parameters p_1 and p_2 are shown in Figure 4, where it can be seen particularly in the first and last three natural frequencies that features apparent in the 49-point model are not represented accurately in the 9-point model.

Synthetic experiments were carried out with 100 pairs of random values selected for p_1 and p_2 from a Gaussian distribution with means $[20 \quad 20]$ and covariance matrix $\begin{bmatrix} 9 & 0 \\ 0 & 9 \end{bmatrix}$. The sample means and covariances of the 100 pairs were found to be $[19.5 \quad 19.8]$ and $\begin{bmatrix} 9.11 & 0.14 \\ 0.14 & 8.86 \end{bmatrix}$. The first six natural frequencies of these 100 mass locations were generated as synthetic data from the previously deterministically updated FE model and deterministic model updating was carried out 100 times for the estimation of p_1 and p_2. The starting point for each deterministic update was sampled from a different distribution with the same mean of $[20 \quad 20]$ and covariance terms given by $\begin{bmatrix} 4 & 0 \\ 0 & 4 \end{bmatrix}$. In this way any loss of accuracy in determining the known variability in the mass locations could only be attributed to code uncertainty. The result of this model updating exercise is shown in Figure 5, where again the 49-point model is seen to be superior to the 9-point model. Synthetic and updated results are denoted by red and black '+' signs respectively.

The output scatter plots with superimposed 3σ covariance ellipses shown in Figure 6 were produced by the full FE model with, p_1 and p_2, for each of the 100 samples determined by the two Kriging models. Simulated data are marked in blue and FE outputs are in red. The bar-chart in Figure 7 shows the same information more clearly. It is seen that both Kriging models are able to reproduce the means of the 6 natural frequencies with very good accuracy. The covariances are reproduced less accurately by the 9-point model, especially the variance of the high order natural frequency. Figure 8 shows the means and

covariances of the parameters, p_1 and p_2, where again the mean values are accurately reproduced by both Kriging models and, for the covariances, the 49-point model is superior to the 9-point model, which significantly overestimates the off-diagonal terms. It is clear from Figures 5 to 8 that code uncertainty is virtually eliminated in the 49-point Kriging model but appears to be significant in the 9 point model.

The black '+' points shown in Figure 5 are stochastic model updating results corresponding to the most probable Kriging model. However, the Kriging model includes a Gaussian distribution $\mathcal{N}\left(\overline{\boldsymbol{\theta}},\boldsymbol{\Sigma}_{\theta}\right)$ at each of the 100 measurement points, so that the points shown in black in the figure represent just one sample, albeit the most probable one from $\mathcal{N}\left(\overline{\boldsymbol{\theta}},\boldsymbol{\Sigma}_{\theta}\right)$. The resampling procedure described in Section 4 takes multiple samples from the Gaussian distributions at the points. The result of repeating the resampling process 1000 times is shown in Figure 9 where it is seen that the standard deviations on the mean values and on the output covariance is very small in both cases (9-point and 49-point models). The standard deviation on the input mean and covariance is also very small as shown in Figure 10. It appears from the results shown in Figures 6-8 that the distributions on the updated parameters and on the updated model predictions vary very little when resampling from $\mathcal{N}\left(\overline{\boldsymbol{\theta}},\boldsymbol{\Sigma}_{\theta}\right)$ - the projected input distribution from the Gaussian process. This indicates that the variability introduced by the Kriging Gaussian process present in either of the two cases is very narrow. Therefore a 9-point Kriging model that accurately reproduces the synthetic data seems to be extremely unlikely. A Kriging model with a greater number of points, such as the 49-point model, is clearly required.

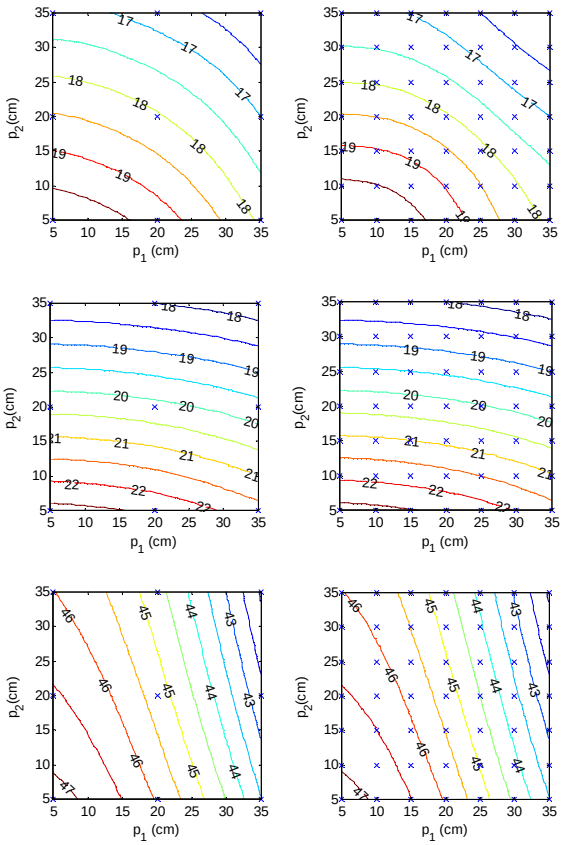

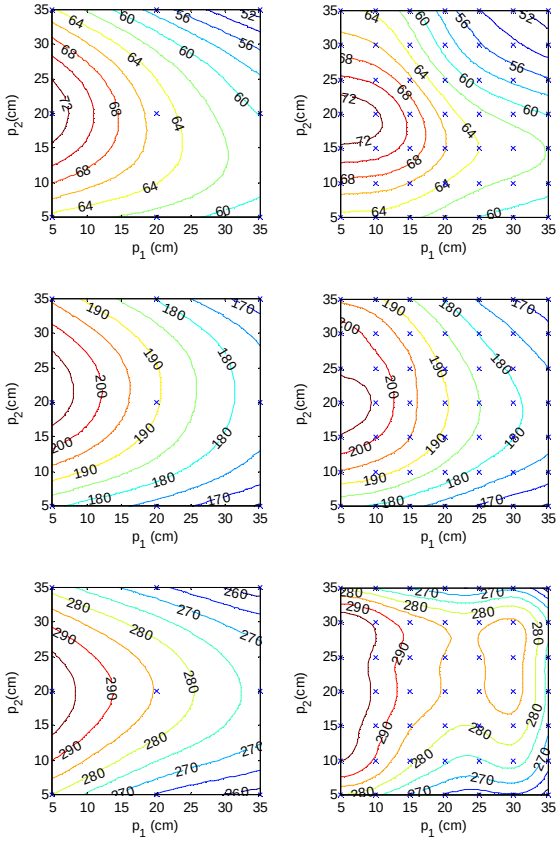

Figure 4: Contours of the Kriging model. Left column: 9-point Kriging. Right column 49-point Kriging. Rows: $f_1, f_2, f_3, f_4, f_5, f_6$. × markers are design point locations. The numbers on the contour lines are the frequency values in Hz.

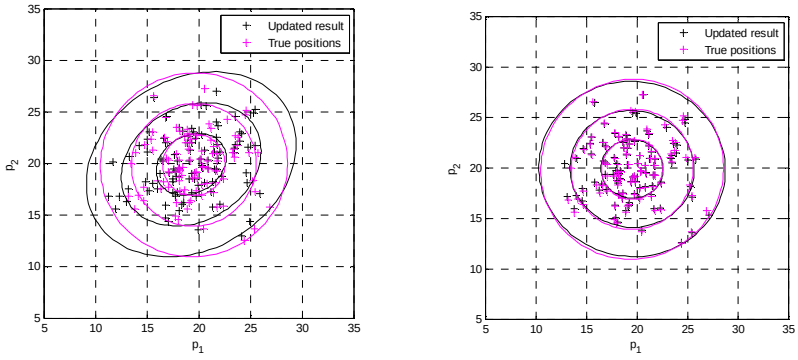

(a) (b)

Figure 5: Updated parameters of 100 synthetic experiments,
(a) 9-design point Kriging model, (b) 49-design point Kriging model

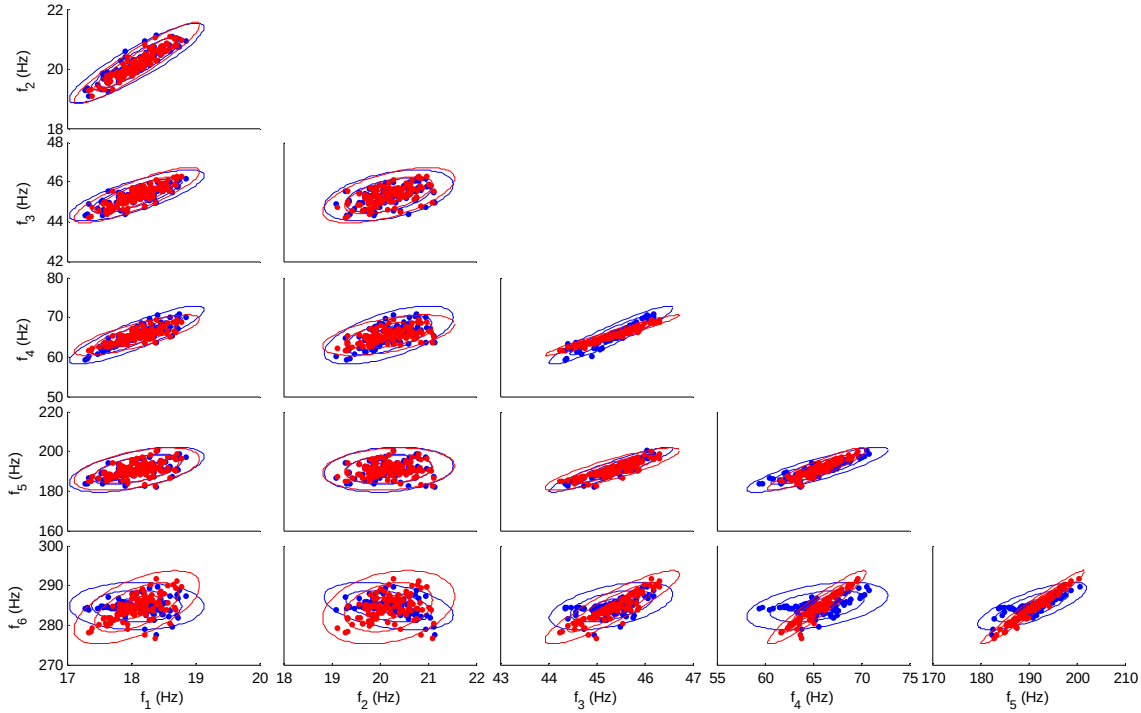

(a)

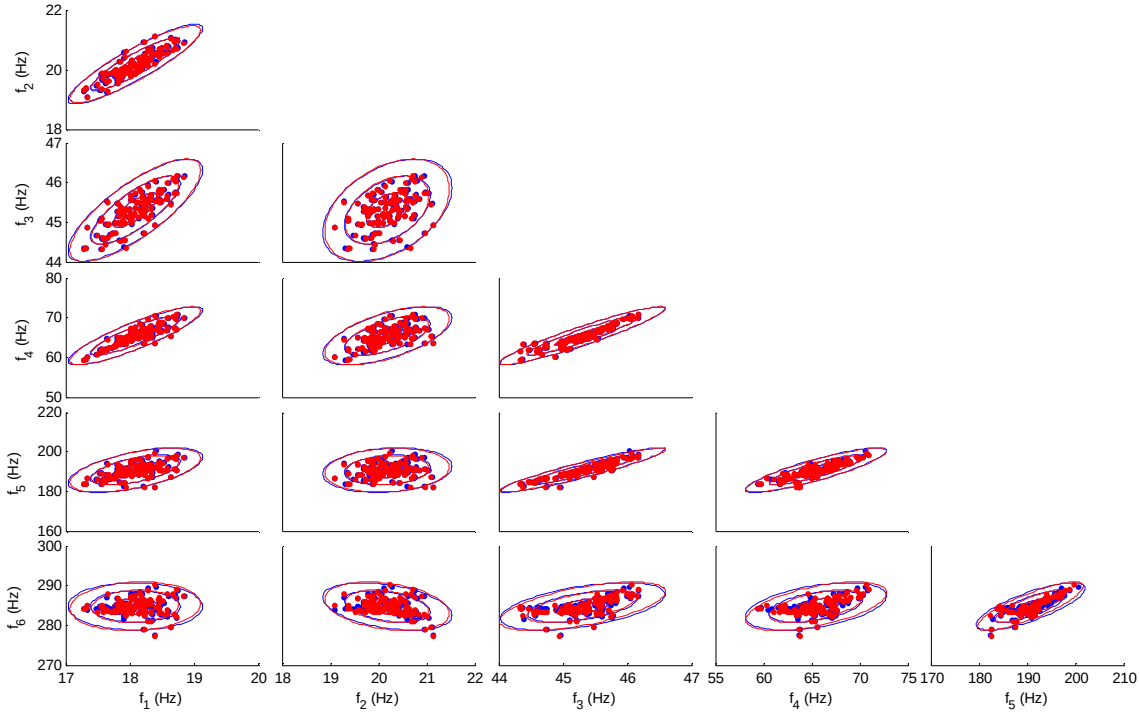

(b)

Figure 6: Updated natural frequencies of 100 synthesis experiments, experiment samples in blue, Kriging samples in red, (a) 9-design point Kriging, (b) 49-design point Kriging

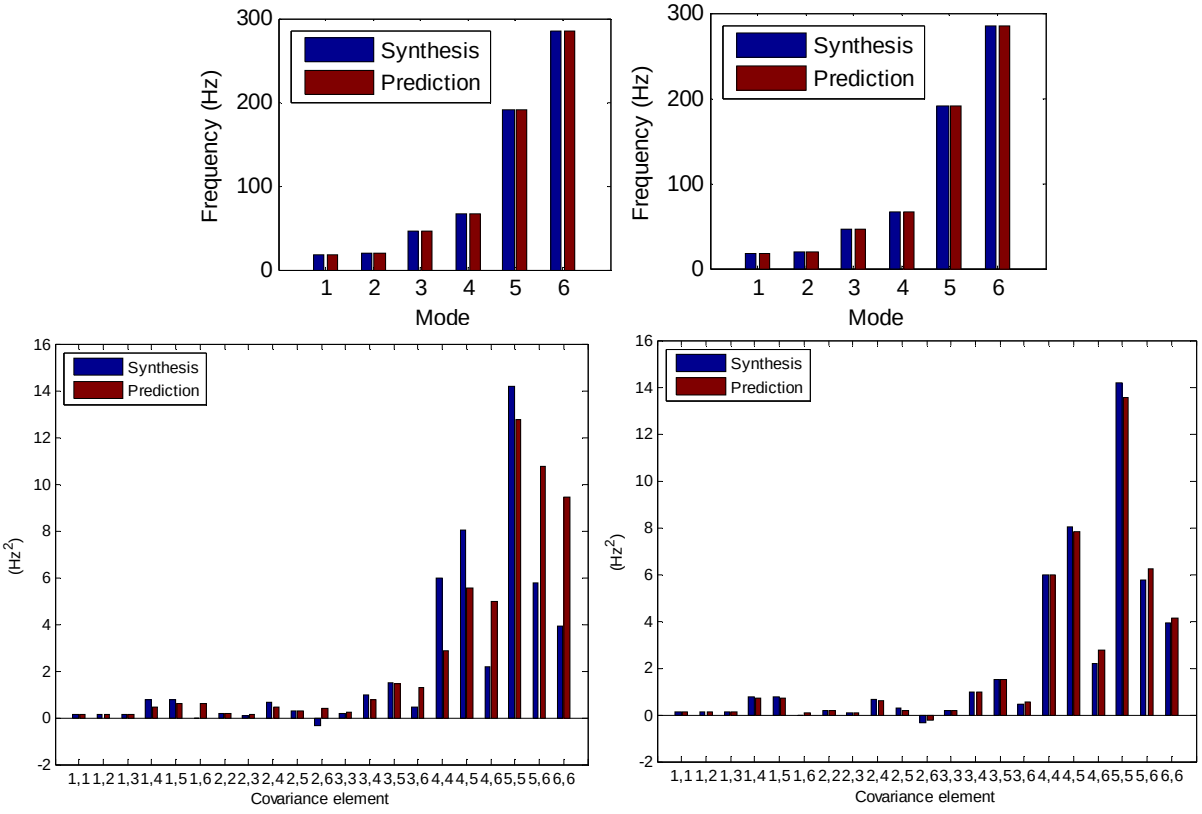

Figure 7: Mean and covariance matrix elements of frequencies computed with updated parameters. Left column: 9-point Kriging. Right column: 49-point Kriging. Row 1: mean values of frequencies. Row 2: covariance matrix elements of frequencies.

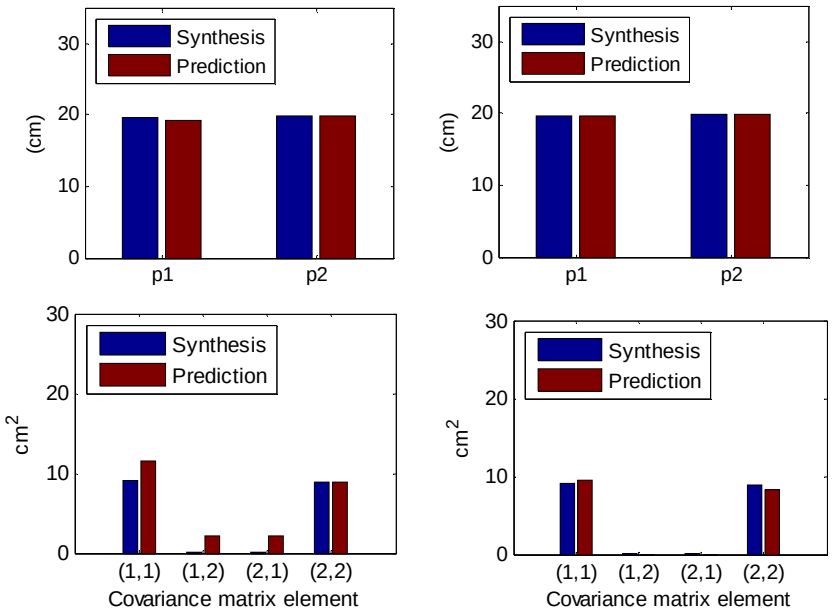

Figure 8: Mean and covariance matrix elements of updated parameters. Left column: 9-point Kriging. Right column: 49-point Kriging. Row 1: mean values of parameters p_1 and p_2. Row 2: covariance matrix elements of parameters p_1 and p_2.

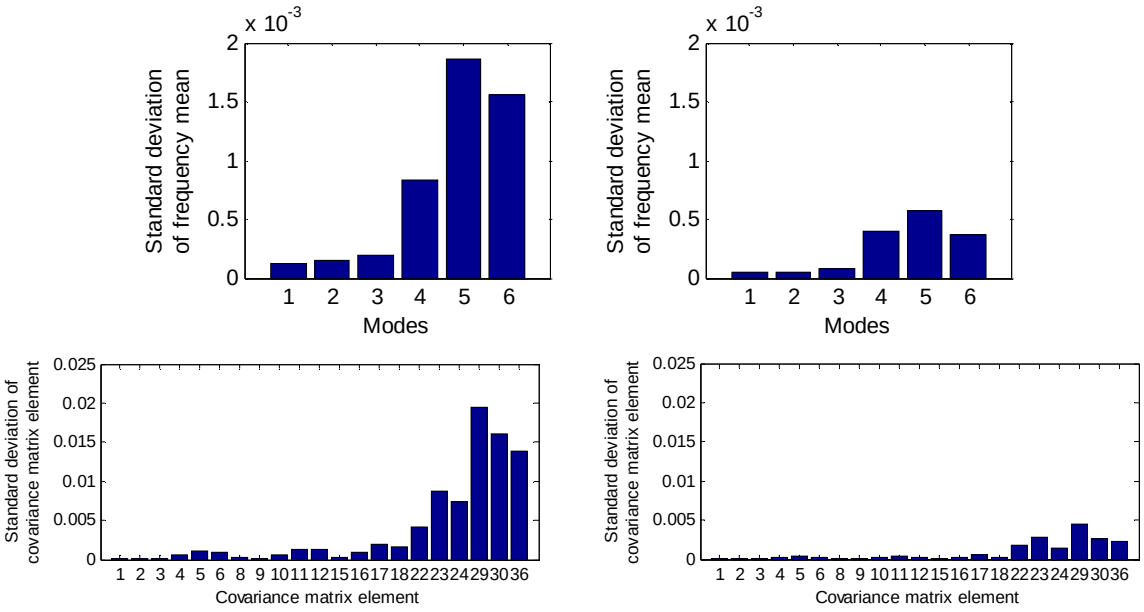

Figure 9: Standard deviations of resampled frequency mean values and covariance elements left column: 9-point Kriging, right column: 49-point Kriging.

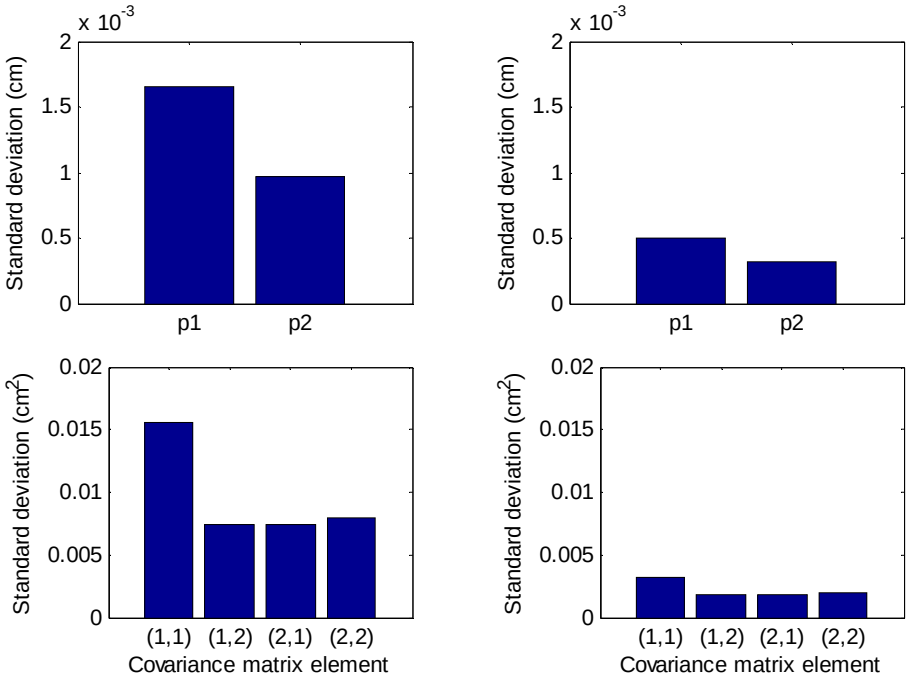

Figure 10: Standard deviations of resampled parameter mean values and covariance elements left column: 9-point Kriging, right column: 49-point Kriging.

10. Step 2: Stochastic model updating using experimental measurements

In this Section, the same 100 pairs (p_1, p_2) are reconsidered, but his time physical measurements are used from the experimental frame. In each of 100 tests the natural frequencies and mode-shapes of the frame

were determined by hammer-impact modal testing. Figures 11 and 12 show the resulting distributions and statistics in the parameter space. Measured and updated results are denoted by red and black '+' signs respectively in Figure 11 together with the 3σ ellipses. The updated results were produced by the 49-point Kriging model, known to possess negligible code uncertainty. The prediction in Figure 12 is seen to reproduce the statistics of p_1 and p_2 with acceptably small errors. Figures 13-15 present the corresponding frequency space result. The 3σ covariance ellipses are shown in Figure 13, in which experimental measurements are marked in blue and prediction results are marked in red.

Outputs from the updated FE model, with Kriging-updated parameters, are shown together with measured frequency data in Figures 13-15. The ellipses in Figure 13 are generally in good agreement, except for the $f_6 - f_4$ ellipse which shows a discrepancy in orientation. This is seen clearly in Figure 15 where all the covariance terms are in good agreement except the (4,6) and (5,5) terms. These errors are probably due to further small deterministic FE errors not completely eliminated by the preliminary deterministic update of the FE model. Never-the-less, the updated parameter distributions are seen to be very good and the updated model is deemed to be acceptable.

Figures 16-18 show the statistics resulting from resampling. They are of the same order of magnitude as their counterparts from the synthetic-data exercise and show the Kriging Gaussian distributions about the mean (most probable) value to be very narrow. Any alternative input function (dashed curve in Figure 2) sampled from the Gaussian process $\mathcal{N}\left(\overline{\boldsymbol{\theta}},\boldsymbol{\Sigma}_\theta\right)$ is likely to have mean values and covariances very close to those in Figure 12. Therefore it is confirmed that the discrepancy in Figure 15 is not due to code uncertainty but to an unresolved modelling error.

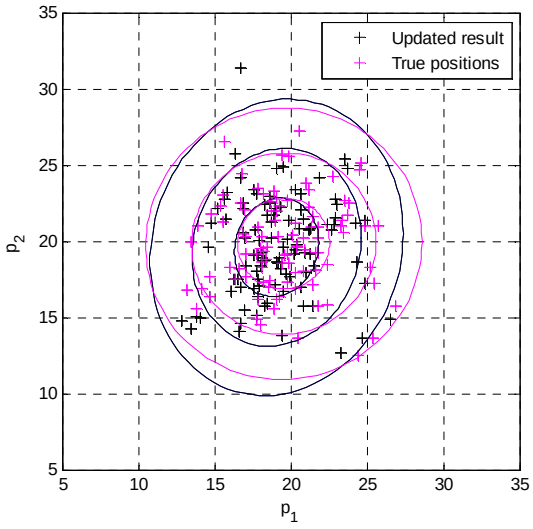

Figure 11: Model updating result – experimental data

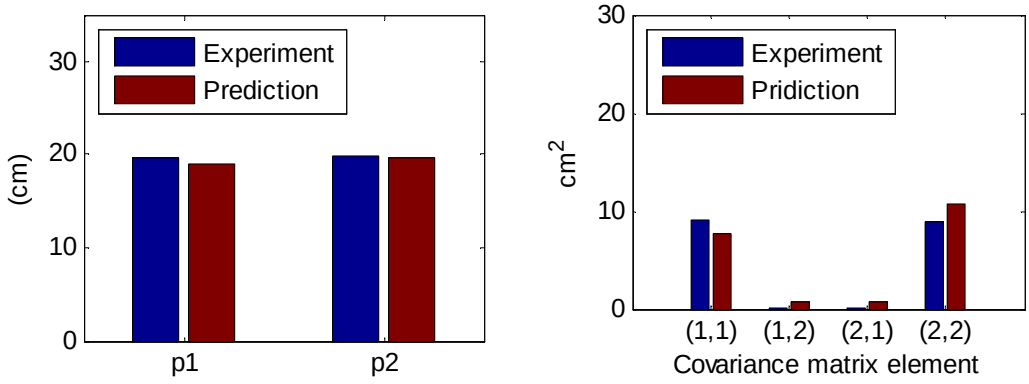

(a) (b)

Figure 12: Comparison of the mean and the covariance matrix elements of updating parameters. (a) The mean value of p_1 and p_2. (b) The covariance matrix elements of p_1 and p_2

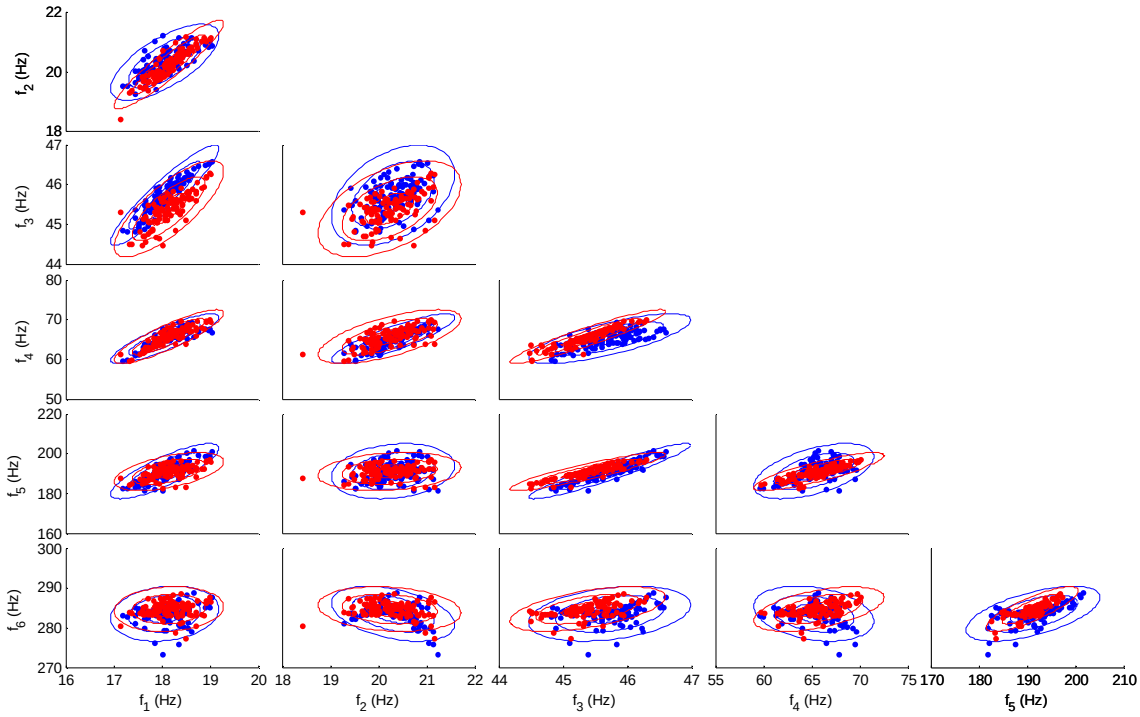

Figure 13: Ellipses of experimental and updated frequencies. Measurements in blue. Predictions in red.

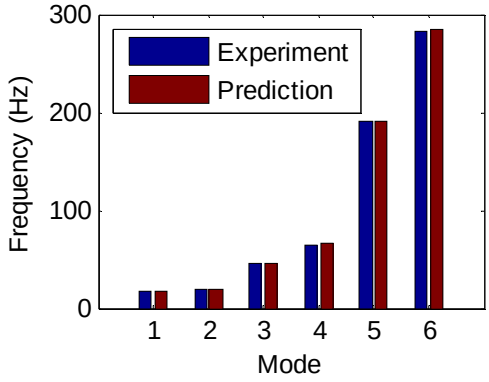

Figure 14: Mean values of frequencies

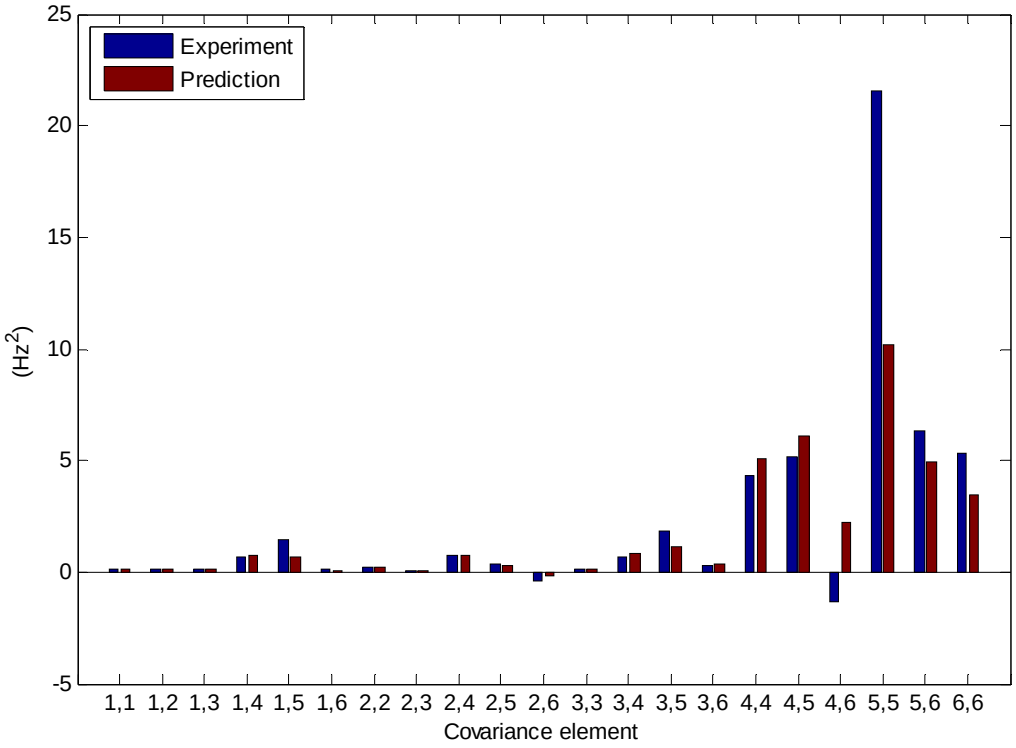

Figure 15: Covariance matrix elements of frequencies

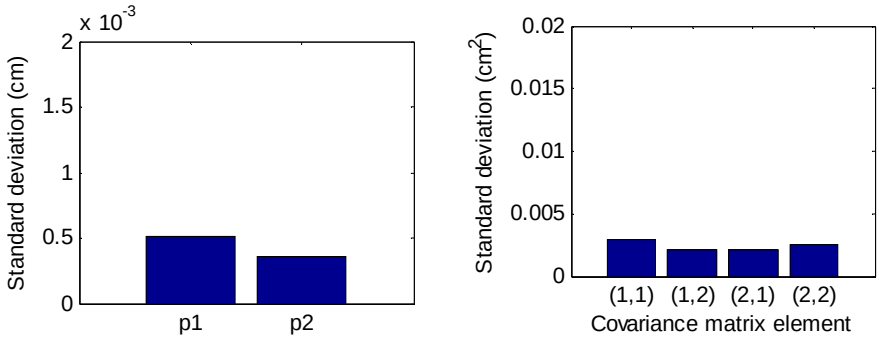

Figure 16: Standard deviations of resampled parameter mean values and covariance matrix elements. (a) Standard deviations of the mean value of p_1 and p_2. (b) Standard deviations of the covariance matrix elements of p_1 and p_2.

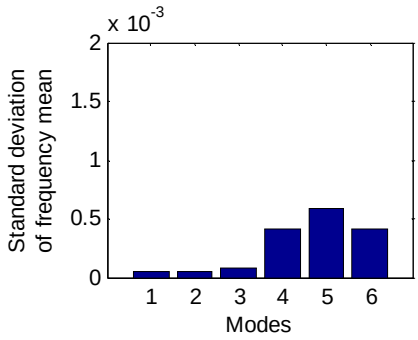

Figure 17: Standard deviation of resampled frequency mean values.

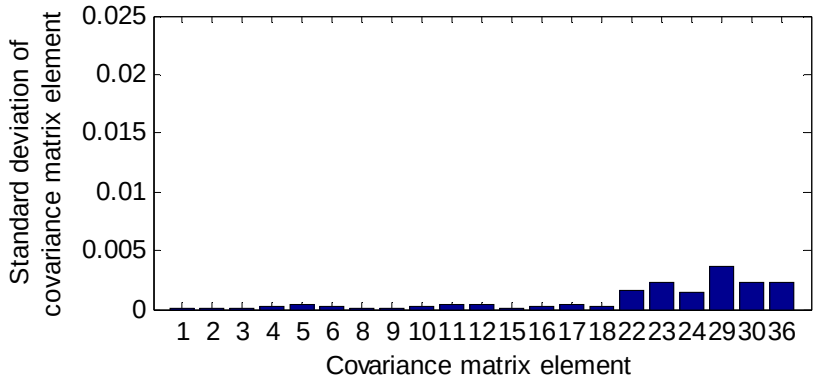

Figure 18: Standard deviation of resampled frequency covariance matrix elements.

11. Conclusions

A procedure to assess the quality of a Kriging model in the representation of structural variability in nominally identical test structures is demonstrated using a laboratory test frame with movable masses. FE models, typified by the frame, generally contain deterministic parameter errors that must be eliminated to prevent contamination of the stochastic model-updating result. Then, having completed a preliminary deterministic update, stochastic model updating can proceed in two steps. In Step 1, a stochastic update is completed with a Kriging model using synthetic measurements from the already deterministically updated model. This allows an assessment of the Kriging model using both output data and inputs obtained by the inverse process of model updating. A resampling technique using the Kriging Gaussian process projected onto the input (parameter) space allows an assessment of other available Kriging functions (not just the most probable one). Re-training is necessary if the Kriging model is deemed to be too far away from the synthetic data and a fully trained model is judged to be free of code uncertainty. Step 2 may them be completed, in which stochastic model updating is carried out using experimental data for correction of the FE model without contamination by code uncertainty. This procedure is demonstrated using the laboratory test frame, code uncertainty is seen to be eliminated and stochastic model updating is completed. Small unresolved deterministic model errors give rise to errors in just two output covariance terms. The input (parameter) statistics are determined to acceptable accuracy.

Acknowledgement

The first author acknowledges the support of the China Scholarship Council and the University of Liverpool.

References

1. Simpson, T.W., et al., *Metamodels for Computer-based Engineering Design: Survey and recommendations.* Engineering with Computers, 2001. **17**(2): p. 129-150.
2. Koch, P.N., et al., *Statistical Approximations for Multidisciplinary Design Optimization: The Problem of Size.* Journal of Aircraft, 1999. **36**(1): p. 275-286.
3. Shao, T., S. Krishnamurty, and G. Wilmes, *Preference-Based Surrogate Modeling in Engineering Design.* AIAA journal, 2007. **45**(11): p. 2688-2701.
4. Gano, S.E., H. Kim, and D.E. Brown II, *Comparison of Three Surrogate Modeling Techniques: Datascape, Kriging, and Second Order Regression,* in *11th AIAA/ISSMO Multidisciplinary Analysis and Optimization Conference*. 2006, American Institute of Aeronautics and Astronautics: Portsmouth, Virginia, USA.
5. Martin, J.D. and T.W. Simpson, *Use of Kriging Models to Approximate Deterministic Computer Models.* AIAA journal, 2005. **43**(4): p. 853-863.

6. DiazDelaO, F.A. and S. Adhikari, *Gaussian process emulators for the stochastic finite element method.* International Journal for Numerical Methods in Engineering, 2011. **87**(6): p. 521-540.
7. Fricker, T.E., et al., *Probabilistic uncertainty analysis of an FRF of a structure using a Gaussian process emulator.* Mechanical Systems and Signal Processing, 2011. **25**(8): p. 2962-2975.
8. Ghoreyshi, M., K.J. Badcock, and M.A. Woodgate, *Accelerating the Numerical Generation of Aerodynamic Models for Flight Simulation.* Journal of Aircraft, 2009. **46**(3): p. 972-980.
9. Khodaparast, H.H., J.E. Mottershead, and K.J. Badcock, *Interval model updating with irreducible uncertainty using the Kriging predictor.* Mechanical Systems and Signal Processing, 2011. **25**(4): p. 1204-1206.
10. Govers, Y., et al., *A comparison of two stochastic model updating methods using the DLR AIRMOD test structure.* Mechanical Systems and Signal Processing, 2015. **52–53**: p. 105-114.
11. Katafygiotis, L.S. and J.L. Beck, *Updating Models and Their Uncertainties. II: Model Identifiability.* Journal of Engineering Mechanics, 1998. **124**(4): p. 463-467.
12. Goller, B., et al., *A stochastic model updating technique for complex aerospace structures.* Finite Elements in Analysis and Design, 2011. **47**(7): p. 739-752.
13. O'Hagan, A., *Bayesian analysis of computer code outputs: A tutorial.* Reliability Engineering & System Safety, 2006. **91**(10–11): p. 1290-1300.
14. Sacks, J., et al., *Design and Analysis of Computer Experiments.* Statistical Science, 1989. **4**(4): p. 409-423.
15. Bastos, L.S. and A. O'Hagan, *Diagnostics for Gaussian Process Emulators.* Technometrics, 2009. **51**(4): p. 425-438.
16. Lophaven, S.N., H.B. Nielsen, and J. Søndergaard, *DACE-A Matlab Kriging toolbox, version 2.0.* 2002.
17. DiazDelaO, F.A., et al., *Stochastic structural dynamic analysis using Bayesian emulators.* Computers & Structures, 2013. **120**: p. 24-32.
18. Krzanowski, W., *Principles of Multivariate Analysis*. Second edition ed. 2000, Oxford, UK: Oxford University Press.
19. Liang, P., *Stochastic Model Updating with Surrogate Models*. 2016, University of Liverpool: Liverpool, UK.